



Published in final edited form as:

Biomed Mater. 2008 September ; 3(3): 034124. doi:10.1088/1748-6041/3/3/034124.

Biocompatibility Implications of Polypyrrole Synthesis Techniques

John M. FONNER^{1,#}, Leandro Forciniti^{2,#}, Hieu Nguyen¹, James Byrne¹, Yann-Fuu Kou¹, Jeja Syeda-Nawaz¹, and Christine E. Schmidt^{1,2,*}

¹Department of Biomedical Engineering, The University of Texas at Austin, Austin, Texas | University Station, MC C0800, Austin, TX 78712

²Department of Chemical Engineering, The University of Texas at Austin, Austin, Texas | University Station, MC C0400, Austin, TX 78712

Abstract

Polypyrrole (PPy) is an inherently conducting polymer that has shown great promise for biomedical applications within the nervous system. However, to effectively use PPy as a biomaterial implant, it is important to understand and reproducibly control the electrical properties, physical topography, and surface chemistry of the polymer. Although there is much research published on the use of PPy in various applications, there is no systematic study linking the methodologies used for PPy synthesis to PPy's basic polymeric properties (e.g., hydrophilicity, surface roughness), and to the biological effects these properties have on cells. Electrochemically synthesized PPy films differ greatly in their characteristics depending on synthesis parameters such as dopant, substrate, and thickness, among other parameters. In these studies, we have used three dopants (chloride (Cl), tosylate (ToS), polystyrene sulfonate (PSS)), two substrates (gold and indium tin oxide-coated glass), and a range of thicknesses, to measure and compare the biomedically-important characteristics of surface roughness, contact angle, conductivity, dopant stability, and cell adhesion (using PC-12 cells and Schwann cells). As predicted, we discovered large differences in roughness depending on the dopant used and the thickness of the film, while substrate choice had little effect. From contact angle measurements, PSS was found to yield the most hydrophilic material, most likely because of free charges from the long PSS chains exposed on the surface of the PPy. ToS-doped PPy films were tenfold more conductive than Cl- or PSS-doped films. X-ray photoelectron spectroscopy studies were used to evaluate dopant concentrations of PPy films stored in water and phosphate buffered saline over 14 days, and conductance studies over the same timeframe measured electrical stability. PSS proved to be the most stable dopant, though all films experienced significant decay in conductivity and dopant concentration. Cell adhesion studies demonstrated the dependence of cell outcome on film thickness and dopant choice. The strengths and weaknesses of different synthesis parameters, as demonstrated by these experiments, are critical design factors that must be leveraged when designing biomedical implants. The results of these studies should provide practical insight to researchers working with conducting polymers, and particularly PPy, on the relationships between synthesis parameters, polymeric properties, and biological compatibility.

Keywords

polypyrrole; conducting polymers; electrochemical synthesis; characterization; biocompatibility; conductivity

[#]JMF and LF contributed equally to this work

*To whom correspondence should be addressed (schmidt@che.utexas.edu; 512-471-1690)

Introduction

Biomaterials must be carefully chosen and manufactured to interact favorably with biological systems. This is especially true within the nervous system, where neurons have been shown to respond to physical (Miller, *et al.* 2002, Dowell-Mesfin, *et al.* 2004, Clark, *et al.* 1990), chemical (Pini 1994, Bray and Hollenbeck 1988, Bentley and O'Connor 1994), and electrical (Schmidt, *et al.* 1997, Ming, *et al.* 2001) cues, in addition to cellular signals. Polypyrrole (PPy), a conducting polymer that is easily synthesized both chemically and electrochemically, has been investigated for use in neural probes (Cui, *et al.* 2003) and as scaffolds to promote axonal elongation for use in nerve guidance channels (Schmidt, *et al.* 1997, Kotwal and Schmidt 2001). Although conducting polymers and PPy in particular are well characterized (Guimard, *et al.* 2007, Sadki, *et al.* 2000, Kaynak 1997, Suárez and Compton 1999, Yuan, *et al.* 1999, Skotheim 1986), there has been little effort made to link biologically relevant polymer properties such as roughness, surface energy, and stability to cellular outcomes. This study seeks to begin filling this gap in research by investigating three commonly used negatively charged dopants: chloride (Cl), tosylate (ToS), and polystyrene sulfonate (PSS).

History of Polypyrrole

PPy is an inherently conducting polymer with interesting electrical properties first discovered and reported in the early 1960s (Bolto, *et al.* 1963). By incorporating anions into the polymer during synthesis, also called doping, the resistivity of PPy is greatly reduced, giving it conductivity within the semiconductor range (Diaz 1981; Diaz and Hall 1983; Diaz and Kanazawa 1983). In general, PPy is an opaque, brittle, amorphous material, although its specific properties are influenced by the dopant (Wynne and Street 1985) and polymerization technique used, as well as a host of other variables. Investigators have explored various dopants, including common ions such as iodine, chloride, polystyrene sulfonate, tosylate, perchlorate, as well as more complex biomolecules such as biotin (George, *et al.* 2006), chondroitin sulphate (Serra Moreno, *et al.* 2007), and nerve growth factor (NGF; Hodgson, *et al.* 1996) with various degrees of success. The dopants chosen for this study, which are Cl, ToS, and PSS, are water soluble, biocompatible, commonly used for biomedical applications, and vary greatly in molecular weight (Schmidt, *et al.* 1997, Wang, *et al.* 2004, George, *et al.* 2005, Guimard, *et al.* 2007). The large variety of ways to synthesize and modify the characteristics of PPy make this material attractive for a wide range of applications, but this flexibility also makes it difficult to select the best synthesis parameters for a specific application.

Polypyrrole Synthesis Parameters

Besides chemical synthesis methods, electrochemical polymerization may be performed by using constant current (galvanostat), constant voltage (potentiostat), or by changing voltage (cyclic voltammetry). Electrochemical synthesis results in a film of doped PPy being deposited on the working electrode (e.g., indium tin oxide (ITO) coated glass slide or gold-coated substrate) of a three electrode setup. The deposition process nucleates around initial points and quickly spreads over the surface of the electrode; the electrode material has a large effect on this adhesion and spreading (Sadki, *et al.* 2000). Previous studies have reported that PPy oligomers adsorb to the electrode once their length makes them insoluble, with subsequent oligomers preferentially adsorbing to the PPy nucleation points (Vernitskaya and Efimov 1997). The doping level, measured as a percentage of anions to monomer units, varies depending on the concentration of anions in solution, but typical values range between 25-30% (Diaz and Kanazawa 1983, Kang, *et al.* 1997). The details of electrochemical synthesis are covered in other papers (Sadki, *et al.* 2000, Vernitskaya and Efimov 1997).

Previous studies have also shown that solvent, pH, substrate, and temperature during synthesis affect the final properties of PPy (Sadki, *et al.* 2000, Carquigny, *et al.* 2008, Kaynak 1997).

Thanks to the solubility of pyrrole monomers, PPy may be synthesized in both aqueous and organic solvents, but comparisons across solvents are difficult because of changes in dopant solubility and pH. Since temperature is usually room temperature and pH is dictated by the solvent, this study focuses on the effects of dopant and substrate - the two synthesis parameters that are most easily manipulated and that have the greatest variability in the literature. Film thickness and roughness were assessed for three dopants, two substrates, and multiple polymerization times, and biocompatibility, conductivity, contact angle, and stability of the created PPy films were compared for the different dopants. All polymerizations were performed at room temperature using constant voltage in aqueous solvent (distilled, de-ionized water) with neutral pH and 0.1 M concentrations of pyrrole and dopant - conditions that may be easily repeated in other laboratories.

Motivation for Polypyrrole as a Biomaterial

The material properties measured in this study were chosen for their relevance to biomedical implants. The roughness of implant surfaces (measured at the nanometer to micrometer scale) affects cell adhesion by changing the surface area perceived by the cell. Contact angle is a relative measure of surface energy, which also strongly affects cell adhesion (Hallab, *et al.* 2001). Conductivity and the stability of dopant/PPy interactions are important for the previously mentioned applications of neural probes and nerve guidance channels, as well as any device using electricity for therapeutic or diagnostic purposes.

To assess biocompatibility, we tested the viability of two cell cultures, rat PC-12 and Schwann cells, on PPy films made with different dopants. PC-12 cells were chosen because of their use in previous studies and their neuron-like behavior, since many proposed uses of PPy are within the nervous system (Cui, *et al.* 2003, Schmidt, *et al.* 1997). Schwann cells were used because their migration into a wound site precedes axon repair, making them an important consideration when designing implants for the peripheral nervous system. Because the phenotypic responses of PC-12 cells and Schwann cells are sensitive to adhesion and surface topography, these two cell types are also good indicators of the effects of subtle differences in the surface energy and roughness of the underlying substrate.

Despite the volume of theoretical studies and characterizations performed for PPy, few studies provide comparative information of biomedically-relevant parameters. By electrochemically synthesizing films with controlled characteristics and examining the resulting cellular response, our goal was to create better, more refined biomaterials for specific applications. We will also provide practical guidelines and observations from our experience in working with PPy films.

Materials and Methods

Materials

Pyrrole, reagent grade, 98%, and the dopants, sodium p-toluene-sulfonate, 95% grade, poly (sodium4-styrene-sulfonate) (PSS), 70,000 Daltons average molecular weight, and sodium chloride, ACS reagent, were purchased from Sigma-Aldrich, St. Louis, MO. Platinum gauze for electrochemical deposition was purchased from Aldrich, Milwaukee, WI. Indium tin oxide (ITO)-coated unpolished float glass slides (25 × 75 × 0.5 mm, 30-60 Ω) were purchased from Delta Technologies, Stillwater, MN, and frosted pre-cleaned microscope slides were purchased from Stuart Scientific, Greensburg, Pennsylvania. Isopropanol (1-Propanol), 99%, was purchased from Sigma-Aldrich. Fisherbrand plates and Pasteur pipettes were used throughout the experiments. All other chemicals used were 98% reagent grade or better.

Polypyrrole Synthesis

To create gold-coated slides, an Edwards Auto 500 thermal evaporator was used to deposit chromium and gold onto untreated, frosted, pre-cleaned microscope slides. The slides were further cleaned by sonication in distilled, deionized water for 10 minutes, followed by sonication in isopropanol, and were stored in isopropanol until use. Between 4-8 nm of chromium was first thermally deposited on the surface of the microscope slide, followed by thermal deposition of 40 nm of gold.

Next, pyrrole monomer was purified by passing it through an aluminum oxide column. Three dopant types (Cl, ToS, PSS) were used to synthesize three types of polypyrrole films on two different substrates (ITO and gold). For the synthesis, an aqueous solution of 0.1 M pyrrole and 0.1 M dopant anions was used in combination with a three electrode electrochemical setup. Since PSS is a poly-anionic molecule capable of doping PPy in many locations, the anion concentration (0.1 M) of PSS was used for comparison with the other two mono-anionic species (Cl, ToS) rather than the molecular concentration (~283 μ M).

For the three-electrode setup, a gold-coated or ITO-coated slide with an accessible surface area of 7.5 cm² (25 mm slide width by 30 mm) was used as the working electrode. A platinum mesh (20 mm by 30 mm) served as the counter electrode, and a saturated calomel electrode was used as the reference electrode. An oxidizing potential of 720 mV supplied by a potentiostat (CH Instruments, electrochemical analyzer) was used for all PPy polymerization reactions. The passage of charge was recorded to test its correlation with thickness, as initially proposed by Diaz and Hall. (1983).

The macroscopic surface area of each film was measured using a ruler and the films were then rinsed extensively with deionized water for 10 minutes. Once properly rinsed, the films were kept under vacuum overnight to dry.

Physical Property Characterization of PPy Films

Film thickness and roughness measurements were performed using a Dektak 6M Stylus Profiler (Veeco) profilometer. Two parallel scratches were made on the PPy film approximately 2 mm apart, and the average step height was calculated between the scratches on the film. The roughness was calculated using Equation 1:

$$R_q = \frac{1}{L} \sqrt{\int_0^L y(x)^2 dx} \quad [1]$$

where L is the distance between the scratches and y(x) is the average height above or below the median line for any given position. For all of our profilometer scans, we maintained an in-plane sampling resolution of 0.5 μ m as defined by the scan speed and data sampling rate. The thickness measurement accuracy of the profilometer is reported as +/- 0.1 nm. The films were then tested for surface energy using a goniometric setup, with a Navitar CV-M30 camera and Edmund Optics test stand. 5 μ L of reagent grade water was placed on the surface of the film, and 5 images were acquired 15-30 seconds after the droplet touched the surface of the polypyrrole. The average contact angle from these images was calculated.

Electrical Conductivity Characterization of PPy Films

Electrical conductivities of the polypyrrole films, ranging in thickness from 0.29 - 1.6 μ m, were measured using a Jandel four-point probe (1.0 mm tip spacing) with a CH Instruments, electrochemical analyzer and a Lucas Labs resistivity test stand. The sheet resistivity was then calculated using Equation 2:

$$R_s = \frac{4.5324 * V}{I} \quad [2]$$

where I [amperes] is the current passed between the two inner electrodes, V [volts] is the voltage across the two outer electrodes, and R_s [Ohms/square] is the sheet resistivity. To accurately measure electrical conductivity of PPy, it is essential to remove the conducting polymer films from the underlying conducting gold or ITO substrates. From our experience, the most effective method for removing the films from the conducting substrates is using double-sided tape and to place the exposed side of the tape onto the surface of a glass slide, a technique with some precedence in the literature (Mabrouk 2005). Other possible methods we have tested in the past include using a razor blade to peel the films off the conducting substrate or backing the film with poly-dimethylsiloxane (PDMS) to aid in removal. When using a razor blade the fragile films tend to roll up on themselves because of their high surface energy. In using PDMS, we found that PDMS can leach through the film and prevent good contact with the four-point probe. Removal with double-sided tape was a practical method to move the film to an insulating substrate without causing damage to the film. From our comparisons, the presence of the tape did not alter the conductivity of the film.

Using the thickness, t [cm], taken from previous profilometer measurements, the conductivity, σ [Siemens/cm], for a given film was then calculated using Equation 3:

$$\sigma = \frac{1}{R_s * t} \quad [3]$$

Dopant Stability

X-ray photoelectron spectrographs (XPS) and conductance measurements were taken over a two week period for films submerged in either 1 X PBS (pH ~ 7.4) or DDI water (~ 18 M Ω) to determine the dopant stability of PPy films. PBS was chosen because it resembles physiological salt concentrations. For XPS, eight thick films (84 mC/cm²) were electrochemically synthesized for each of the three dopants used in this manuscript. Each film was then washed for five minutes in DDI water and dried in a vacuum desiccator overnight. Immediately after drying, small portions of each film were removed and measured using XPS to calculate a baseline doping level. The remainders of each of the films were placed in a Petri dish and submerged in either PBS or DDI water. Two, seven, and fourteen day time points were also taken by removing additional portions of the films at each time point. Core level X-ray emissions were measured for N(1s), S(2p), Cl(2p), and Na(1s) for each of the samples. The doping ratio was then calculated as a ratio between the dopant anion (S or Cl) and pyrrole ring nitrogen (N). In each sample, low sodium levels verified that proper washing of the films had taken place.

For conductance measurements, eight thick films (84 mC/cm²) were electrochemically synthesized for each of the three dopants used in this manuscript. All films were allowed to dry in a vacuum desiccator overnight. Films were removed with double-sided tape, cut into equal halves, and put into a watertight well setup. The well setup was created by putting a polydimethylsiloxane (PDMS) layer on a glass slide and then stacking on top the PPy film, two silver wires along opposing edges of the PPy film, a second layer of PDMS with a 1 x 1.5 cm square removed from the center, and finally a polycarbonate well. All layers were held together by wrapping the edges with electrical tape. This setup ensured a watertight seal to minimize leakage while allowing conductance measurements to be taken *in situ*. Initial conductance measurements were taken, the wells were filled with PBS or DDI water, and a second set of conductance measurements were obtained to account for changes in conductance due to the solution. Over a two week period of time, additional measurements were acquired to observe the conductance decay. All measurements were taken by passing a small DC current through the silver wires and measuring the resulting voltage. The direction of the current was then switched and the voltage measured again. The strength of the current used was always

adjusted to produce a voltage between 10 and 100 mV. The conductance value was then determined by dividing the current by the average voltage.

Cell Culture and Cell Viability Characterization

Schwann cells and rat pheochromocytoma PC-12 cells were cultured on PPy to determine film property effects on cell viability. Both cell types were cultured on six films, thin (10.7 mC/cm²) and thick (84 mC/cm²) films for each dopant (Cl, ToS, PSS) on ITO slides. For the PC-12 cell experiment, sterile polycarbonate wells with inner dimensions of 1.0 × 1.5 cm² (made in-house) were secured onto the films with UV-sterilized high vacuum grease (Dow Corning, Midland, MI). For the Schwann cell experiments, wells with inner diameters of 9 mm were made from sterile Press-to-Seal Silicone Isolators (Grace Bio Labs, Bend, OR) and were secured onto films with UV-sterilized high vacuum grease. Before culturing cells, the wells attached to polypyrrole films on glass were sterilized for 30 minutes using UV exposure and washed for 10 minutes using 1 mL phosphate buffered saline (PBS) for the large wells and 100 μL PBS for the small wells.

Rat pheochromocytoma PC-12 cells from American Type Culture Collection were selected for this study because of their ability to differentiate into a neuronal phenotype after exposure to nerve growth factor (NGF). PC-12 cells were maintained in F12K medium with 10% horse serum and 5% fetal bovine serum on collagen-coated polystyrene tissue culture dishes (2.75 μg rat tail Collagen I per 10cm diameter dish, Sigma-Aldrich, St. Louis, MO). Cells were exposed to 50 ng/mL NGF (2.5S Murine, Promega, Madison, WI) for 5 days prior to seeding on PPy substrates, changing medium on the third day, and maintained in a humid 37°C, 5% CO₂ incubator. Cells were detached using 0.25% Trypsin-EDTA, resuspended and triturated before seeding the cells at 20,000 cells per well (13,000 cells/cm²). Cultures grown on PPy were maintained in 300 μL of medium containing serums, NGF, and 1% penicillin/streptomycin/amphotericin B (PSA) for 24 hours.

Schwann cells were also selected for this study because Schwann cell migration precedes axon regrowth at a neural injury site. Cells were isolated from P4 neonatal rat sciatic nerves using a modified Brockes method to obtain 95% cell purity as measured by S-100 immunostaining. Schwann cells were maintained in high glucose DMEM medium with 10% fetal bovine serum, 3 μg/mL of bovine pituitary extract (Invitrogen, Carlsbad, CA), and 2 μM forskolin (Sigma-Aldrich, St. Louis, MO) on 10 cm diameter poly-L-lysine (PLL) coated tissue culture dishes (2 μg/cm², Fisher Scientific, Pittsburgh, PA). Cells were cultured to 70-80% confluency, then detached using 0.25% Trypsin-EDTA and seeded at 6000 cells per well (9,500 cells/cm²). Cultures grown on polypyrrole were maintained in 100 μL of medium containing serum, supplements, and 1% PSA for 24 hours.

Measurement of PC-12 and Schwann cell viability on polypyrrole was assessed using a luminescent ATP detection assay (CellTiter Glo, Promega, Madison, WI). The wells were aspirated and then incubated with 100 μL of fresh medium and 100 μL of detection reagent. After 30 minutes, the supernatant was pipetted into a 96-well plate and analyzed with a luminescent microplate reader (FLx800, BioTek Instruments, Inc., Winooski, VT). Calibration curves for luminescent values correlating to cell numbers were created for each experiment.

Leached products from thick PPy substrates were used to examine cytotoxic effects on Schwann cells. Sterile Silicon Isolator wells were secured onto thick PPy films and onto PLL-coated tissue culture dishes with UV-sterilized high vacuum grease. Wells on PPy films and Schwann cells seeded on PLL plates were both incubated 24 hours at 37°C with 100 uL of media containing serum and supplements. Following the 24 hour incubation, media was aspirated from the Schwann cell cultures and replaced with media incubated on the thick PPy

films. After cells were cultured for another 24 hours, cell viability was measured using an ATP assay.

Statistics and Error Propagation

In all calculations, the general relation of propagation of uncertainty was used. To determine statistical significance, an n of three or greater was used for all characterization techniques. Standard error was reported for all relevant figures. Two-tailed Student t -tests were performed for each of the values of interest for cell studies, contact angle studies, and conductivity studies. Statistically significant groups in Figures 3, 5 and 8 are identified at the 0.05 level with different letters (A, B, or C); groups with the same letter are not statistically significant. Only comparisons that had a p -value of 0.05 or less were considered statistically significant.

Results and Discussion

PPy Film Thickness

Film thickness is an important parameter to consider for cell studies either *in vivo* or *in vitro*. The electrochemical polymerization of PPy was reported (Diaz and Hall 1983) to be a stoichiometric process, with between 2.2 and 2.4 electrons passed per monomer unit polymerized. The slight variability in the process depends on the doping level of the film (Diaz and Hall 1983). Unfortunately, subsequent studies suggest that other factors may affect the “yield” or efficiency of this reaction, such as oligomers that remain in solution and undesired side reactions (Vernitskaya and Efimov 1997). With these findings in mind, our goal was to assess how well film thickness may be predicted using standard electrochemical synthesis techniques.

Figure 1 illustrates the correlation between film thickness and charge passed per unit area in a log-log plot. A linear trend was fitted to the data with the y-axis intercept set to zero. The linear fits for ToS- and PSS-doped films have similar slopes for both substrates and R^2 values greater than 0.83. Chloride-doped films produced the steepest slope (seen as a parallel line shifted upwards in a log-log plot) for both conductive substrates, demonstrating that Cl-doped films grow much thicker than PSS- or ToS-doped films. Chloride-doped film growth also had very low correlation with charge passed, yielding R^2 values of 0.53 for gold and 0.77 for ITO substrates. This translates to an average error of 26%, 36%, and 183% between the calculated thickness and the actual thickness for PSS-, ToS-, and Cl-doped films, respectively. Perhaps more interesting, however, is the observation that for the same amount of charge passed, Cl-doped films are over twice as thick as PSS- or ToS-doped films when polymerized on a gold substrate and roughly eight times as thick when polymerized on ITO.

Theoretical, stoichiometric calculations were performed based on the equation given by Stankovic, *et al.* (1994) to compare experimental thickness measurements to their predicted values. The slopes of the regression lines in Figure 1 along with theoretical values are shown in Table 1. Since electropolymerization of PPy requires the passage of two electrons per pyrrole ring plus an electron for each dopant ion incorporated, the thickness, Th , of the films per charge passed per unit area should be given by:

$$\frac{Th}{Q_0/A} = \frac{(M_m + yM_a)}{d(2/\gamma + y)F} \frac{p}{(p-1)} \quad [4]$$

where Q_0 is the charge passed, A is the surface area of the working electrode, d is the density of doped PPy, y is the degree of polymerization, and M_m and M_a are the molecular weights of the pyrrole repeat unit and the dopant anion respectively. Gamma (γ) represents the efficiency of the applied current and p is the degree of polymerization. The slopes reported in Table 1 use the approximations that $\gamma=1$, that p is very large, that $y=0.3$, and that $d=1.5$ g/mol. Experimental

observations for the film growth of ToS- and PSS-doped PPy are relatively near stoichiometric predictions, but Cl-doped PPy films were thicker than predicted, especially for higher charge passed per area values. Previous studies using ClO_4 as the dopant have also reported films thicker than theoretical predictions (Stankovic, *et al.* 1994), postulating decreases in density as the primary cause.

It is well known that synthesis current densities (charge passed per area per time) have significant effects on film morphology and conductivity (Maddison and Unsworth 1989, Schmeisser, *et al.* 1993, Stankovic, *et al.* 1994). The main difference between the substrates used, ITO and gold, is conductivity. As a result of the higher conductivity of gold, electrochemical synthesis on gold substrates tends to occur faster than on ITO. Figure 2 shows that the current density is indeed greater for those films synthesized on gold than those synthesized on ITO for all dopants. Furthermore, Figure 1 shows a tight distribution on both substrates for all dopants except chloride. Other studies (Bufon, *et al.* 2005, Schmeisser, *et al.* 1993) also report that current density during synthesis affects chain length and chain disorder, which may explain some of the variability observed when correlating thickness to charge passed for Cl-doped films. The optimal current density found by Stankovic for tosylate-doped films of 1 mA/cm^2 aligns well with the median value found for films synthesized on gold substrates.

Contact Angle Measurements

The water contact angle of smooth surfaces is a relative measure of the surface energy of the material (Yekta-Fard and Ponter 1992). Materials with higher surface energies (i.e., materials that are more hydrophilic) exhibit better cell adhesion (Hallab, *et al.* 2001). Water contact angles for relatively smooth films (less than 50 nm root mean squared roughness in our case) for each of the dopants were used to compare surface energy as a function of dopant type. These smooth samples were chosen since roughness is a source of error for contact angle measurements (Yekta-Fard and Ponter 1992). Figure 3 shows that PPy films doped with PSS, a polyanionic molecule, have more hydrophilic surfaces than those films doped with monoanionic dopants such as Cl and ToS. This result is expected and is likely explained by the fact that free charges are present in the longer strands of PSS in the PSS-doped films whereas no such free charges exist in the Cl- and ToS-doped films.

Surface Roughness

Since roughness is an important consideration for cell adhesion, changes in roughness as a result of different dopants and different thicknesses must be taken into account. We noticed that film growth on our two substrates, gold and ITO, were distinct, so comparisons between substrates were also expected to show differences. Also, since the roughness of an amorphous material inherently contains a high level of variance, this analysis is descriptive of general trends and cannot be used to reproducibly generate films with a specific roughness.

Figure 4 shows how roughness increases with thickness for the three dopants used; in addition, three typical thickness profiles of thick films obtained using profilometry are shown. PSS-doped PPy was by far the smoothest material, with roughness remaining almost constant for all thicknesses. Qualitatively, while observing the polymerization on the substrate, the PSS-doped PPy film grew evenly across the substrate. The fact that PSS-doped PPy adsorbs uniformly on the electrode (with more nucleation points) may be caused by the large PSS dopant polyanion adsorbing to the electrode and providing a favorable surface for further PPy adsorption (Vernitskaya and Efimov 1997). For thin samples, ToS-doped PPy also maintains essentially constant roughness, but samples thicker than a few hundred nanometers increase in roughness as they become thicker. Chloride-doped PPy films were much rougher than PSS- and ToS-doped PPy, and roughness rapidly increased with thickness. Roughness values

obtained are within the range of previously published values obtained by scanning tunneling microscopy (Chainet and Billon 1998). From observation, Cl-doped PPy films deposited unevenly during polymerization and usually started from only a few nucleation points. When comparing the roughness of samples between the gold and ITO substrates, no significant change in roughness was observed (data not shown). Although differences in the growth and macroscopic uniformity of the films were observed, this did not significantly affect the micrometer scale roughness. Mabrouk (2005) also report no correlation between substrate and surface morphology on the nanometer scale based on atomic force microscopy (AFM) data.

Conductivity Measurements

Figure 5 shows the conductivity of PPy films for the three dopants tested. ToS-doped PPy films have conductivities ten times higher than either PSS-doped or Cl-doped films. The conductivity measured for tosylate-doped films correlates well with the $60 \Omega^{-1}\text{cm}^{-1}$ value reported by Maddison and Unsworth (1989). Films that were doped with PSS had slightly higher conductivities than Cl-doped films. Since ToS is fundamentally a monomer unit of PSS, the observed difference in conductivities between PSS- and ToS-doped films is likely the result of lower doping levels in PSS-doped films. Due to steric hindrances, only a fraction of the charges on a strand of PSS will be able to effectively dope PPy aromatic rings. The remaining charges, although entrapped in the film, will not increase the conductivity of the film. For ToS ions, however, it is possible for every incorporated ion to dope the film. The difference in conductivity between Cl-doped and ToS-doped films is likely caused by multiple factors. Cl has roughly a sixth of the mass of ToS, and diffuses out of the films quickly, as supported by the XPS and conductivity measurements reported in Figure 8. The washing and drying protocol implemented likely reduced the conductivity of the Cl-doped films more than that of ToS-doped films. Our own experience and other previous studies (Kuhn, *et al.* 1995, Chehimi and Abdeljalil 2004) indicate that the conductivity of ToS-doped films is more stable than Cl-doped films. As reported by Vernitskaya and Efimov (1997), the size and nucleophilicity of the dopant anion itself affects the electrical conductivity as well, making ToS-doped PPy more conductive.

Dopant Stability

PPy owes its high conductivity to the dopant ions that serve as an electrical bridge between polymer molecules. Loss of stability in these doping interactions, therefore, leads to a loss in conductivity. For long-term, conductive implants, such as neural probes, stable doping is of paramount importance. Two techniques were employed to test PPy doping stability from an electrical perspective and a chemical composition perspective. In the first, PPy films were stored at room temperature in PBS and DDI water for 0-14 days and their conductance was measured daily. In the second technique, PPy films stored at room temperature in PBS and DDI water for zero, two, seven, and fourteen days were analyzed using XPS measurements for nitrogen, sodium, sulfur and chlorine. Since PPy contains one nitrogen atom per monomer unit, the doping ratio of PPy can be calculated by dividing the number of dopant ions (either sulfur or chloride in our case) by the number of nitrogen atoms. In the context of XPS measurements, the ratio of atomic concentration percentages was used to calculate the doping ratio.

Figure 6 shows XPS and conductance data for PPy films in water and PBS. For PSS-doped films, it should be noted that XPS measurements capture each anion in the molecule whether it is actually doping the film or just sterically bound to the surface. XPS data indicate that some PSS was lost over the first few days, but then stabilized. Conductance, however, continued to decrease over time, indicating that even though anions were entrapped within the film, they slowly lost their doping interactions. The continued degradation in conductance for PSS-doped films can likely be attributed to the reduction of the nitrogen in the PPy backbone. The conductance and XPS data show that both ToS- and PSS-doped films decayed faster in PBS than in DDI water. This is believed to be caused by ions in solution that may either displace

dopant ions or extinguish the charge interactions between PPy and dopant. The Cl-doped PPy conductance decayed more rapidly in DDI water than in PBS because the diffusion gradient existing in water was greater than in PBS solution. Unfortunately, this was not verified by the XPS data, as the chloride atomic composition in the polymer effectively reached zero for both solutions within two days.

Cell Studies

PPy films of two thicknesses, thin (10.7 mC/cm² of charge passed, ~150 nm average thickness) and thick (84 mC/cm², ~650 nm average thickness), and with each of the three dopants were compared in terms of their ability to support cell growth. Figure 7a shows phase contrast images of PC-12 cells cultured on the three different PPy substrates. Qualitatively this figure shows that differences in cell spreading did occur for our different substrate conditions. PC-12 cells are able to clump together and survive through cell-cell interactions without attaching to the substrate, which can partially mask differences in cell viability. As such Schwann cells were chosen as a comparative study. Figure 7b shows corresponding phase contrast images of Schwann cells. Different cell morphologies can qualitatively be seen for each of the dopants used (inset). Schwann cells grown on PSS-doped PPy seem to prefer a thin, spindle-like morphology, whereas films doped with the other two dopants seem to prefer alternative more spread morphology. Figures 8a and 8b show that regardless of the cell type used, ToS- and PSS-doped thick films resulted in lower cell adhesion versus their corresponding thin film ($p < 0.05$). Leaching studies were performed with Schwann cells and revealed that medium incubated on thick ToS films resulted in significantly lower cell numbers, confirming that leached dopant molecules may contribute to this decrease (data not shown). Thick chloride films performed as well or better than thin films. As leaching of chloride is not cytotoxic in these quantities, surface roughness may help promote cell adhesion on thick Cl-doped films. Comparing across dopants with PC-12 cells, thick chloride films performed the best ($p < 0.05$). It is interesting to note that negative surface charges on PSS-doped films, which have been known to promote protein adsorption and subsequent cell adhesion (Wittmer, *et al.* 2007, Khorasani, *et al.* 2006, Cai, *et al.* 2006), do not exhibit a significant effect on cell viability of PC-12 cells. On the other hand, for Schwann cells thick PSS-doped PPy films are statistically better than thick ToS-doped films ($p < 0.05$). This is of particular importance as serum proteins such as fibronectin and laminin I and II are known to have significant effects on Schwann cell behavior, including migration (Bailey, *et al.* 1993, Einheber, *et al.* 1993).

Conclusions

PPy is an extremely versatile and promising material for biomedical applications; however, to create a film with tightly controlled properties such as roughness, thickness, and conductivity, the synthesis process must be well refined and the dopants incorporated must be carefully chosen. This study demonstrated that different dopants yield vastly different material properties, which could be important for different biomedical applications. For example, in situations requiring high conductivity, such as electrode coatings, ToS-doped PPy films are far more conductive than PSS- or Cl-doped PPy films. On the other hand, PSS-doped PPy maintains its composition over long periods of time and has a smoother, more hydrophilic surface, making it a good candidate for longer term implants such as neural probes. Chloride has high surface roughness for thicker films, which enhances cell viability, but this material also de-dopes rapidly. With regard to electrochemically synthesizing films of a specified thickness, charge passed per unit area is a marginal indicator of thickness for PSS- and ToS-doped PPy films, but a poor indicator for Cl-doped films. Further investigation is required to explain this variability, but we conclude that the practice of reporting charge passed to infer film thickness has poor accuracy and is insufficient for applications requiring high precision. The cell viability studies showed the importance of both dopant and film thickness, with dopant

leaching and film surface roughness playing dominant roles in the differences observed. As PPy becomes more widely used in a variety of settings with a variety of synthesis parameters used, the most important conclusion may be that careful control over the synthesis process is required to consistently produce films or coatings with desired characteristics.

Acknowledgements

The authors would like to thank Dr. Yangming Sun and Nathalie Guimard for their assistance with XPS. This study was financially supported by the National Institutes of Health (R01 EB004529).

References

- Bailey SB, Eichler ME, Villadiego A, Rich KM. The influence of fibronectin and laminin during Schwann cell migration and peripheral nerve regeneration through silicon chambers. *J Neurocytol* 1993;22:176–184. [PubMed: 8478639]
- Bentley D, O'Connor TP. Cytoskeletal events in growth cone steering. *Curr. Opin. Neurobiol* 1994;4(1): 43–48. [PubMed: 8173324]
- Bolto BA, McNeill R, Weiss DE. Electronic Conduction in Polymers III: Electronic Properties of Polypyrrole. *Aust. J. Chem* 1963;16:1090–1103.
- Bray D, Hollenbeck PJ. Growth cone motility and guidance. *Annu. Rev. Cell Biol* 1988;4:43–61. [PubMed: 2461722]
- Bufon CCB, Vollmer J, Heinzel T, Espindola P, John H, Heinze J. Relationship between chain length, disorder, and resistivity in polypyrrole films. *Journal of Physical Chemistry B* 2005;109:19191–19199.
- Cai K, Frant M, Bossert J, Hildebrand G, Liefeth K, Jandt KD. Surface functionalized titanium thin films: zeta-potential, protein adsorption and cell proliferation. *Colloids Surf B Biointerfaces* 2006;50:1–8. [PubMed: 16679008]
- Carquigny S, Segut O, Lakurd B, Lallemand F, Fievet D. Effect of electrolyte solvent on the morphology of polypyrrole films: Application to the use of polypyrrole in pH sensors. *Synthetic Metals*. 2008In press
- Chainet E, Billon M. In situ study of polypyrrole morphology by STM: effect of the doping state. *J. of Electroanalytical Chemistry* 1998;451:273–277.
- Cehimi MM, Abdeljalil E. A study of the degradation and stability of polypyrrole by inverse gas chromatography, X-ray photoelectron spectroscopy, and conductivity measurements. *Synthetic Metals* 2004;145:15–22.
- Clark P, Connolly P, Curtis ASG, Dow JAT, Wilkinson CDW. Topographical control of cell behaviour: II. Multiple grooved substrata. *Development* 1990;108:635–644. [PubMed: 2387239]
- Cui X, Wiler J, Dzaman M, Altschuler RA, Martin D. *in vivo* studies of polypyrrole/peptide coated neural probes. *Biomaterials* 2003;24:777–787. [PubMed: 12485796]
- Diaz AF. Electrochemical Preparation and Characterization of Conducting Polymers. *Chemica Scripta* 1981;17:145–148.
- Diaz AF, Hall B. Mechanical-Properties of Electrochemically Prepared Polypyrrole Films. *Ibm Journal of Research and Development* 1983;27:342–347.
- Diaz, AF.; Kanazawa, KK. Polypyrrole: An Electrochemical Approach to Conducting Polymers. In: Miller, JS., editor. *Extended Linear Chain Compounds*. 3. Plenum Press; New York and London: 1983. p. 417-441.
- Dowell-Mesfin NM, Abdul-Karim MA, Turner AMP, Schanz S, Craighead HG, Roysam B, Turner JN, Shain W. Topographically modified surfaces affect orientation and growth of hippocampal neurons. *J. Neural Eng* 2004;1:78–90. [PubMed: 15876626]
- Einheber S, Milner TA, Giancotti F, Salzer JL. Axonal regulation of Schwann cell integrin expression suggests a role for alpha 6 beta 4 in myelination. *J Cell Biol* 1993;123:1223–1236. [PubMed: 8245127]
- George PM, Lyckman AW, LaVan DA, Hegde A, Leung Y, Avasare R, Testa C, Alexander PM, Langer R, Sur M. Fabrication and biocompatibility of polypyrrole implants suitable for neural prosthetics. *Biomaterials* 2005;26:3511–3519. [PubMed: 15621241]

- George PM, LaVan DA, Burdick JA, Chen C, Liang E, Langer R. Electrically Controlled Drug Delivery from Biotin-Doped Conductive Polypyrrole. *Adv. Mater* 2006;18:577–581.
- Guimard N, Gomez N, Schmidt CE. Conducting Polymers in Biomedical Applications. *Progress in Polymer Science* 2007;32:876–92.
- Hallab NJ, Bundy KJ, O'Connor K, Moses RL, Jacobs JJ. Evaluation of Metallic and Polymeric Biomaterial Surface Energy and Surface Roughness Characteristics for Directed Cell Adhesion. *Tissue Engineering* 2001;7(1):55–71. [PubMed: 11224924]
- Hodgson AJ, John MJ, Campbell T, Georgevich A, Woodhouse S, Aoki T, Ogata N, Wallace GG. Integration of biocomponents with synthetic structures—Use of conducting polymer polyelectrolytes composites. *SPIE* 1996;2716:164–176.
- Kang, ET.; Neoh, KG.; Tan, KL. Photoelectron Spectroscopy of Conductive Polymers. In: Nalwa, HS., editor. *Handbook of Organic Conductive Molecules and Polymers*. John Wiley & Sons; New York: 1997. p. 121-181.
- Kaynak A. Effects of Synthesis Parameters on the Surface Morphology of Conducting Polypyrrole Films. *Materials Research Bulletin* 1997;32(3):271–285.
- Khorasani MT, Moemenbellah S, Mirzadeh H, Sadatnia B. Effect of surface charge and hydrophobicity of polyurethanes and silicone rubbers on L929 cells response. *Colloids Surf B Biointerfaces* 2006;51:112–119. [PubMed: 16872811]
- Kotwal A, Schmidt CE. Electrical stimulation alters protein adsorption and nerve cell interactions with electrically conducting biomaterials. *Biomaterials* 2001;22(10):1055–1064. [PubMed: 11352099]
- Kuhn HH, Child AD, Kimbrell WC. Toward Real Applications of Conductive Polymers. *Synthetic Metals* 1995;71:2139–2142.
- Mabrouk PA. Oxidative electropolymerization of pyrrole from neat monomer solution. *Synthetic Metals* 2005;150:101–105.
- Maddison DS, Unsworth J. Optimization of Synthesis Conditions of Polypyrrole From Aqueous Solutions. *Synthetic Metals* 1989;30:47–55.
- Miller C, Jeftinija S, Mallapragada S. Synergistic Effects of Physical and Chemical Guidance Cues on Neurite Alignment and Outgrowth on Biodegradable Polymer Substrates. *Tissue Engineering* 2002;8(3):367–378. [PubMed: 12167224]
- Ming G, Henley J, Tessier-Lavigne M, Song H, Poo M. Electrical Activity Modulates Growth Cone Guidance by Diffusible Factors. *Neuron* 2001;29:441–452. [PubMed: 11239434]
- Pini A. Axon Guidance: Growth cones say no. *Current Biology* 1994;4(2):131–133. [PubMed: 7953512]
- Sadki S, Schottland P, Brodie N, Sabouraud G. The mechanisms of pyrrole electropolymerization. *Chem. Soc. Rev* 2000;29:283–293.
- Schmeisser D, Naarmann H, Göpel W. The two-dimensional structure of polypyrrole films. *Synthetic Metals* 1993;59:211–221.
- Schmidt CE, Shastri VR, Vacanti JP, Langer R. Stimulation of neurite outgrowth using an electrically conducting polymer. *Proc. Natl. Acad. Sci* 1997;94:8948–8953. [PubMed: 9256415]
- Serra Moreno J, Panero S, Artico M, Filippini P. Synthesis and characterization of new electroactive polypyrrole-chondroitin sulphate A substrates. *Bioelectrochemistry*. 2007Online availability (Nov 13 2007) ahead of print
- Skotheim, TA., editor. *Handbook of conducting polymers. II*. Marcel Dekker; New York: 1986.
- Stankovic R, Pavlovic O, Vojnovic M, Jovanovic S. The Effects of Preparation Conditions on the Properties of Electrochemically Synthesized Thick-Films of Polypyrrole. *European Polymer Journal* 1994;30:385–393.
- Suárez MF, Compton RG. In situ atomic force microscopy study of polypyrrole synthesis and the volume changes induced by oxidation and reduction of the polymer. *Journal of Electroanalytical Chemistry* 1999;462:211–221.
- Vernitskaya TV, Efimov ON. Polypyrrole: a conducting polymer; its synthesis, properties and applications. *Russian Chemical Reviews* 1997;66(5):443–457.
- Wang X, Gu X, Yuan C, Chen S, Zhang P, Zhang T, Yao J, Chen F, Chen G. Evaluation of biocompatibility of polypyrrole in vitro and in vivo. *Journal of Biomedical Materials Research* 2004;68A(3):411–422. [PubMed: 14762920]

- Wittmer CR, Phelps JA, Saltzman WM, Van Tassel PR. Fibronectin terminated multilayer films: protein adsorption and cell attachment studies. *Biomaterials* 2007;28:851–860. [PubMed: 17056106]
- Wynne KJ, Street GB. Poly(pyrrole-2-ylum tosylate): Electrochemical Synthesis and Physical and Mechanical Properties. *Macromolecules* 1985;18:2361–2368.
- Yekta-Fard M, Ponter AB. Factors affecting the wettability of polymer surfaces. *Journal of Adhesion Science and Technology* 1992;6(2):253–277.
- Yuan YJ, Adeloju SB, Wallace GG. In-situ electrochemical studies on the redox properties of polypyrrole in aqueous solutions. *European Polymer Journal* 1999;35:1761–1772.

(a) = ITO (b) = Gold

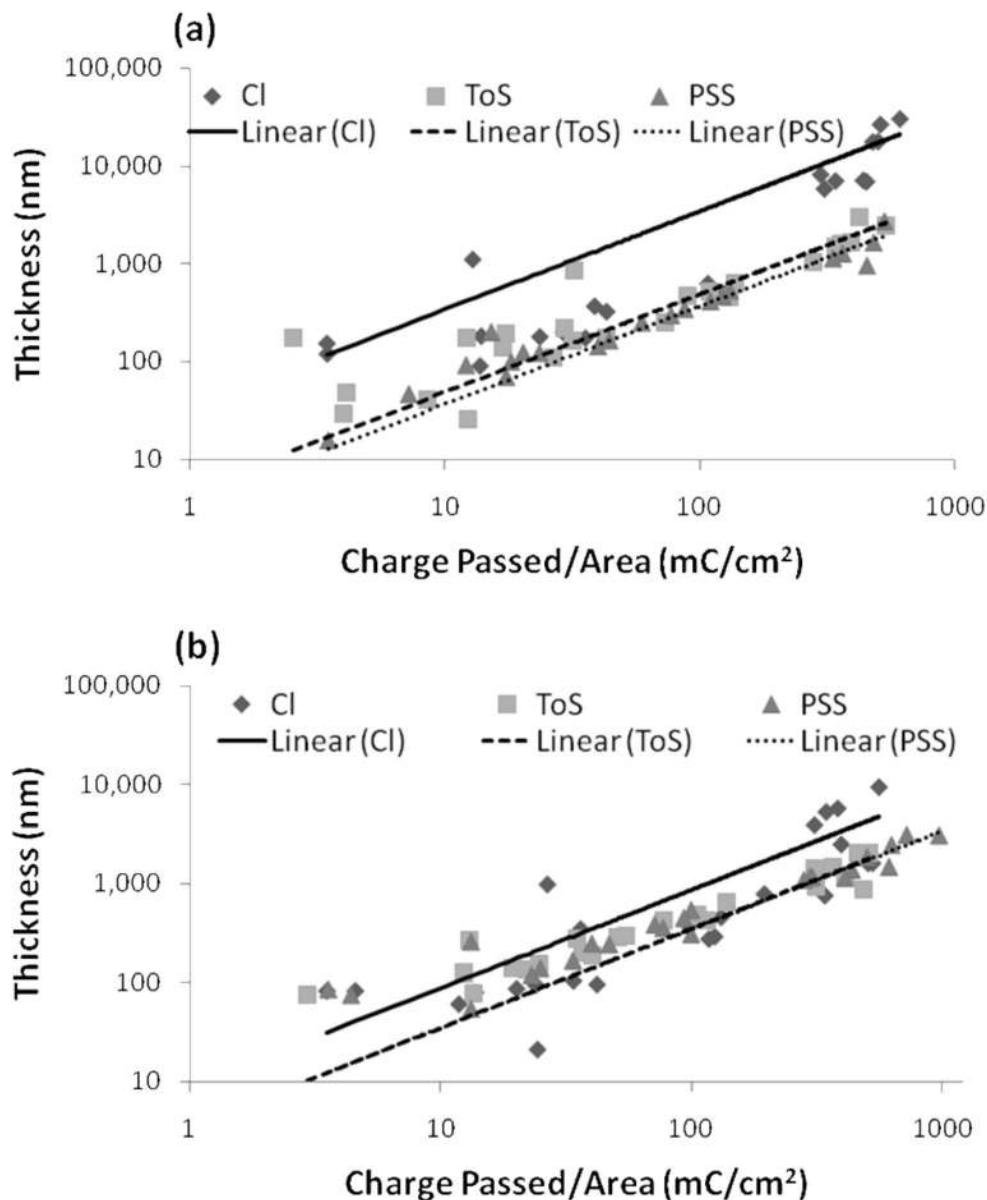


Figure 1. Correlation Between PPy Film Thickness and Charge Passed per Area

Thicknesses in nanometers versus charge passed per area are plotted in a log-log plot for all three dopants for both ITO (a) and gold (b) conductive substrates. A linear correlation was observed for all three dopants for each of the conductive substrates, but Cl-doped films exhibited high variability, demonstrating that charge passed is not a good indicator of thickness for Cl-doped films. ToS and PSS dopants yielded similar slopes, whereas Cl-doped films yielded slopes eight fold (ITO; a) and two fold (gold; b) higher, indicating that the relationship between thickness and charge passed is highly dependent on both dopant and substrate. For all dopants, films grown on ITO films were thicker than films grown on gold for equal quantities

of charge passed per unit area. This change in yield may be related to deposition rate (also measured as current densities).

light gray = ITO dark gray = Gold

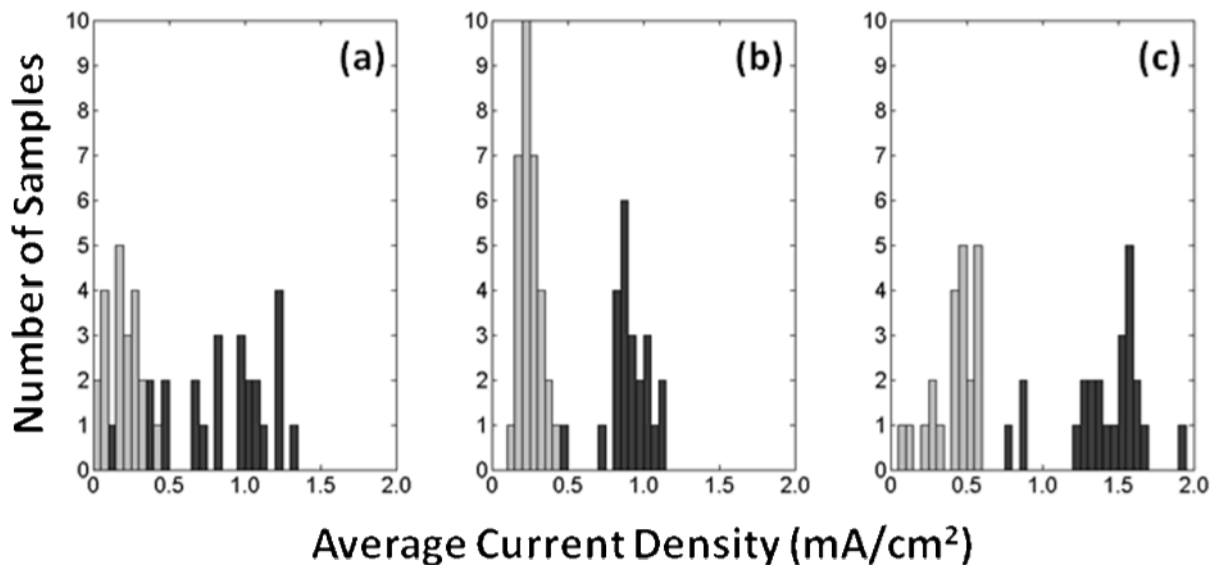


Figure 2. Histograms of the Average Current Density (charge passed/(area*time)) in Electrochemical Syntheses

Syntheses on ITO (light gray) and gold (dark gray) are shown for Cl-doped films (a), ToS-doped films (b), and PSS-doped films (c). Gold electrode substrates consistently resulted in higher current density and thus higher deposition rates, which may impact the yield or efficiency of the amount of material polymerized for a given charge passed. The higher variability in the current density during Cl-doped film synthesis may relate to high variability of film thicknesses observed. All syntheses were performed under the same conditions: 0.1 M concentration of pyrrole and dopant ions, room temperature, neutral pH, and aqueous solvent (distilled, de-ionized water).

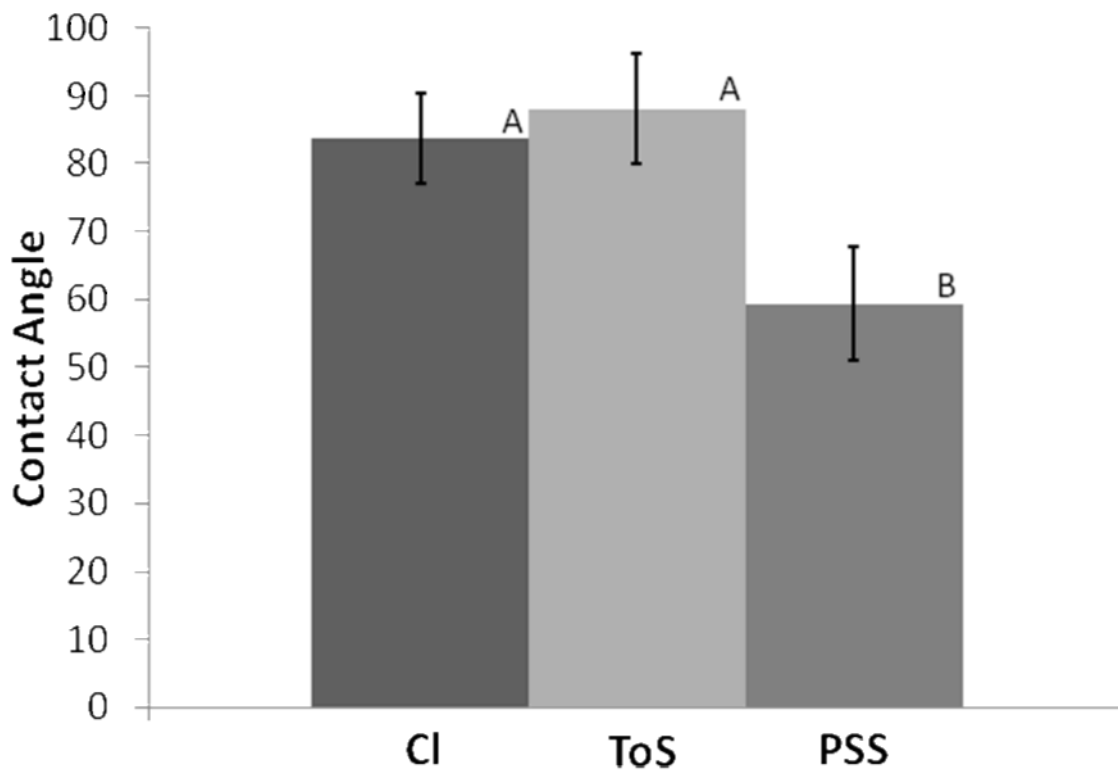


Figure 3. Contact Angles for PPy Films

The contact angle for PPy films with Cl and ToS dopants are statistically more hydrophobic than PSS-doped PPy films. This is likely a result of the free charges found on the longer PSS strands in PSS-doped films. Statistically significant groups are identified at the 0.05 level with different letters (A or B) above each bar graph. (For Cl and ToS, n=4. For PSS, n=7)

(a), (d) = Cl; (b), (e) = ToS; (c), (f) = PSS

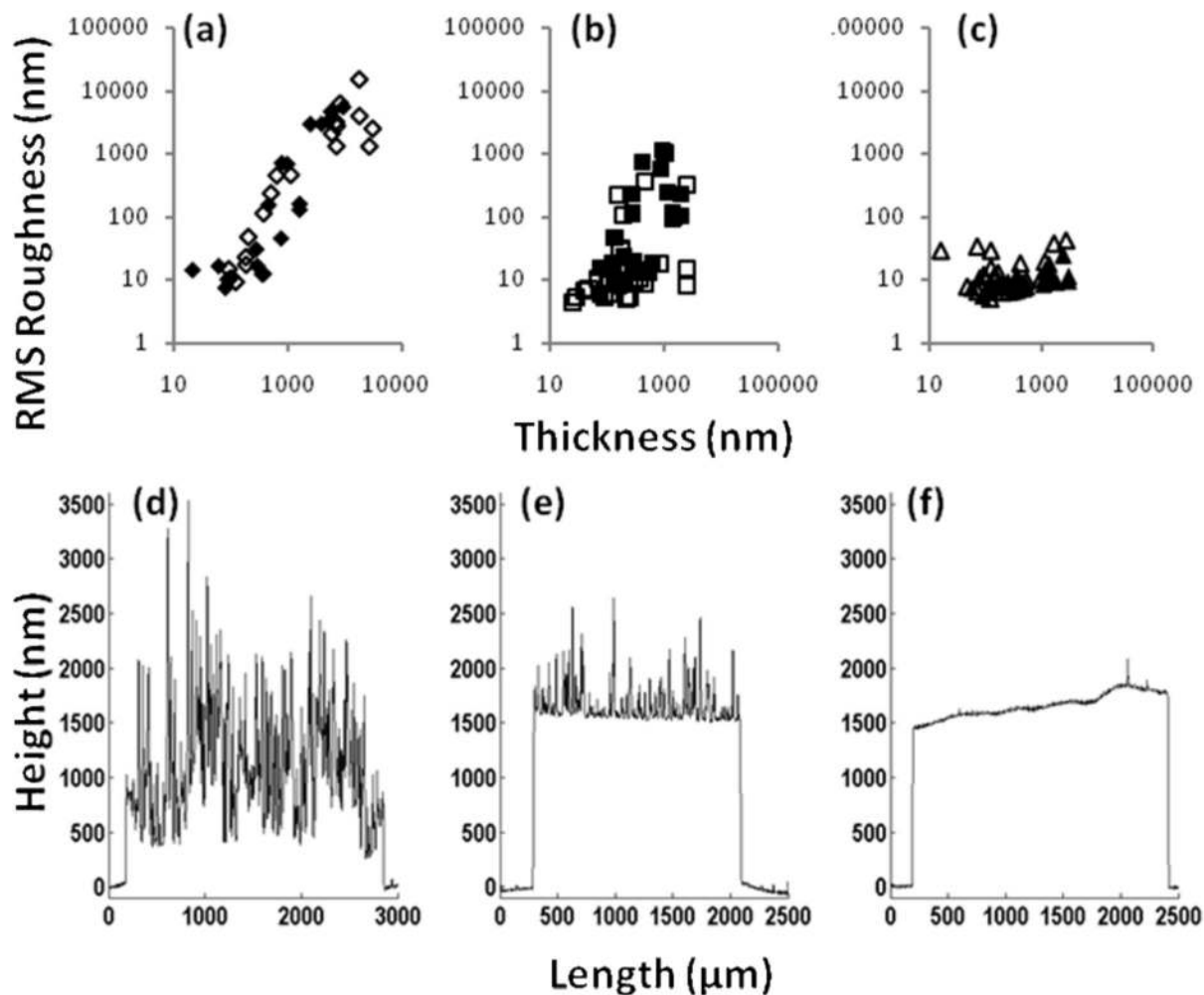


Figure 4. PPy Film Roughness

Roughness values at various thicknesses for the three dopants: Cl (a), ToS (b), and PSS (c). The roughness of Cl-doped films increases with thickness, whereas the roughness of PSS-doped films remains almost constant for all thicknesses measured. Films synthesized on ITO substrates are denoted as hollow symbols, and films on gold substrates are shown as solid symbols. No significant difference was observed between these groups. Typical profilometer measurements of Cl-doped PPy (d), ToS-doped PPy (e), and PSS-doped PPy (f) are shown as a qualitative example of the differences in topography.

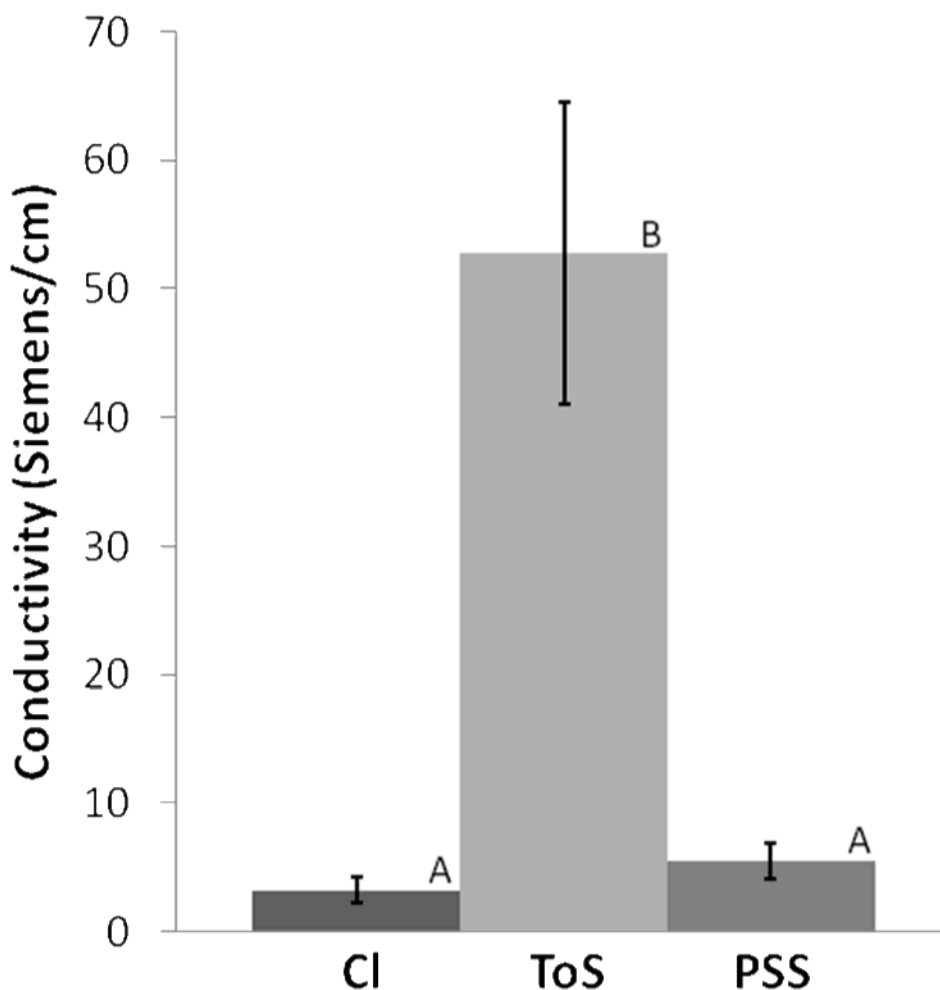


Figure 5. Conductivity as a Function of Dopant

Conductivity measurements of doped PPy films demonstrate that ToS-doped films are ten times more conductive than PSS- or Cl-doped films. PSS-doped films have a slightly higher conductivity than Cl-doped films. Since PSS is fundamentally a polymerized form of ToS, this difference in conductivity most likely relates to the entrapment of a proportion of PSS ions that do not actually dope PPy. For a PSS molecule in a PPy film, steric hindrances only allow a fraction of the anions on the molecule to contribute to the conductivity of the film. ToS ions, in contrast, are able to move more freely to allow stronger doping interactions with PPy. On the other hand, the small size and high solubility of chloride make it a less stable dopant, and the washing steps of our protocol may have disrupted the doping interactions, resulting in de-doping and thus less conductive Cl-doped films. Statistically significant groups are identified at the 0.05 level with different letters (A or B) above each bar graph. (n = 5)

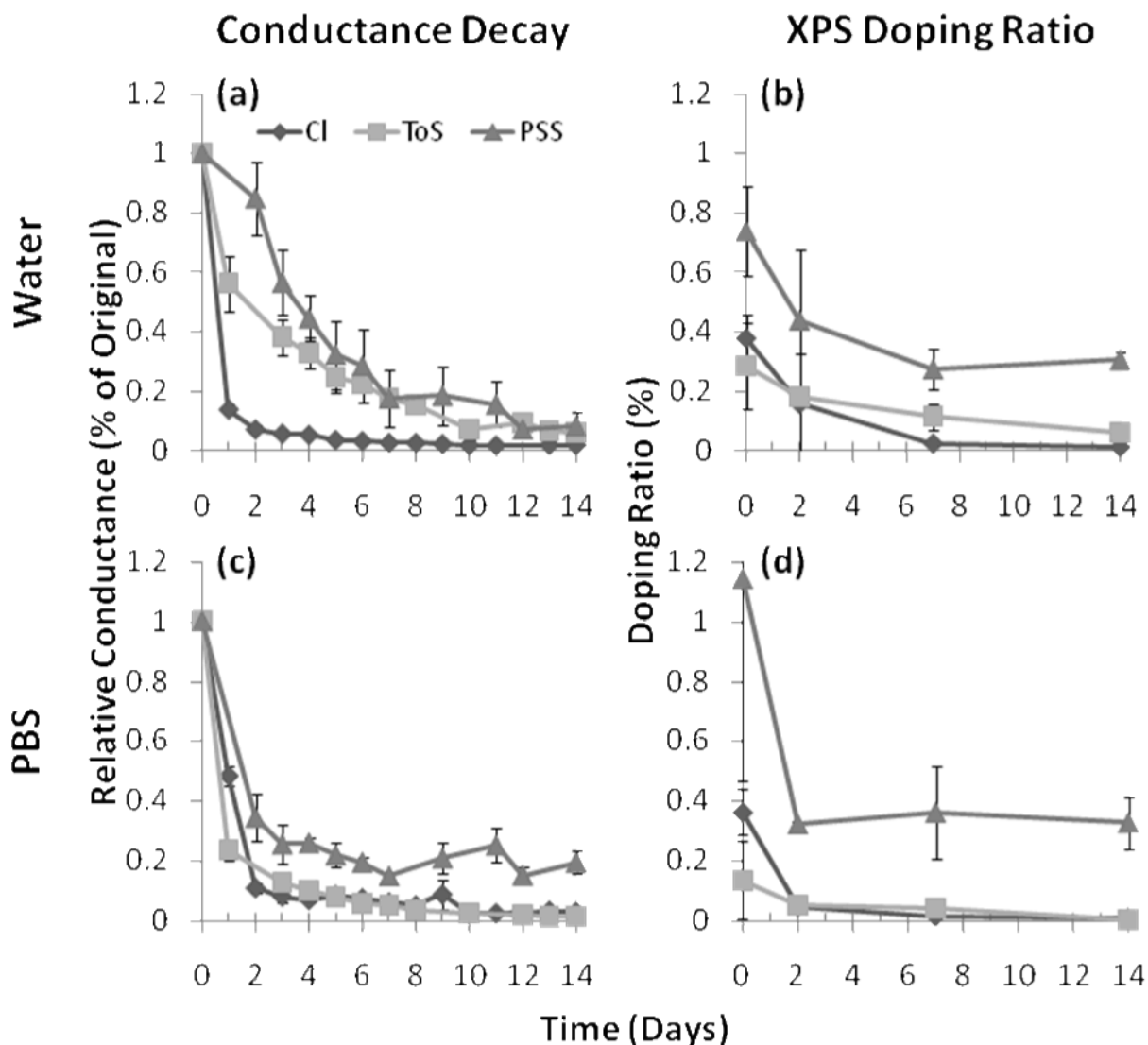


Figure 6. Dopant Stability in Physiological Conditions

Conductance measurements of thick PPy films (84 mC/cm^2) doped with each of the three dopants (Cl, ToS, and PSS) immersed in either DDI water (a) or PBS (c) are shown over a fourteen day time period. The doping ratios (ratio of dopant ions to pyrrole rings) calculated from X-ray photoelectron spectrographs show chemical composition data for films stored in water (b) or PBS (d). For PSS, both XPS and conductance data show a decrease over the first few days with conductance data continuing to decrease over the entire period even though the chemical composition stabilizes. This suggests that even though PSS molecules remain entrapped within the film they slowly lose their doping interactions. The conductance and XPS data show that both ToS- and PSS-doped films decay faster in PBS than in DDI water because of salt interactions. Because of the larger diffusion gradient, Cl-doped films degraded faster in DDI water than in PBS.

a: PC 12 Cells

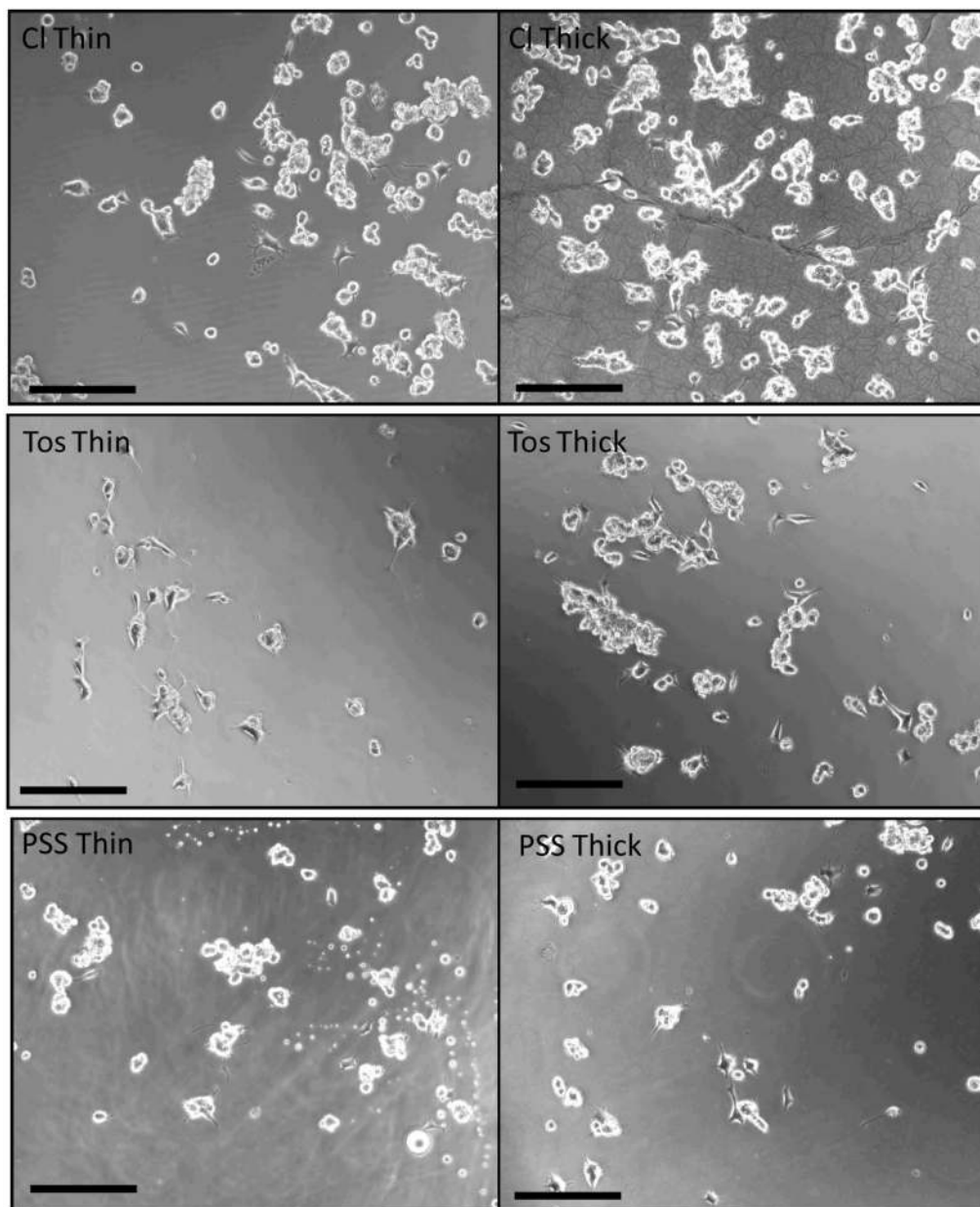


Figure 7. Phase Contrast Images of Cell Cultures on PPy Films

(a) PC-12 cells were cultured for 24 hours on sterilized films and phase contrast images were taken for both thin films (10.7 mC/cm^2 of charge passed) and thick films (84 mC/cm^2). Qualitatively this figure shows that differences in cell spreading did occur for our different substrate conditions. PC-12 cells tend to aggregate and survive as a result of cell-cell interactions without attaching to the substrate, which can partially mask differences in cell viability. Scale bar = $250 \mu\text{m}$. (b) Schwann cells were cultured for 24 hours on sterilized films and phase contrast images were taken for thin films (10.7 mC/cm^2 of charge passed). Different cell morphologies are observed for each of the dopants used (inset). Schwann cells grown on

PSS-doped PPy adopted a thin, elongated bipolar morphology whereas cells on Cl- and ToS-doped films exhibited a spread morphology. Scale bar = 250 μm . Inset Scale bar = 50 μm .

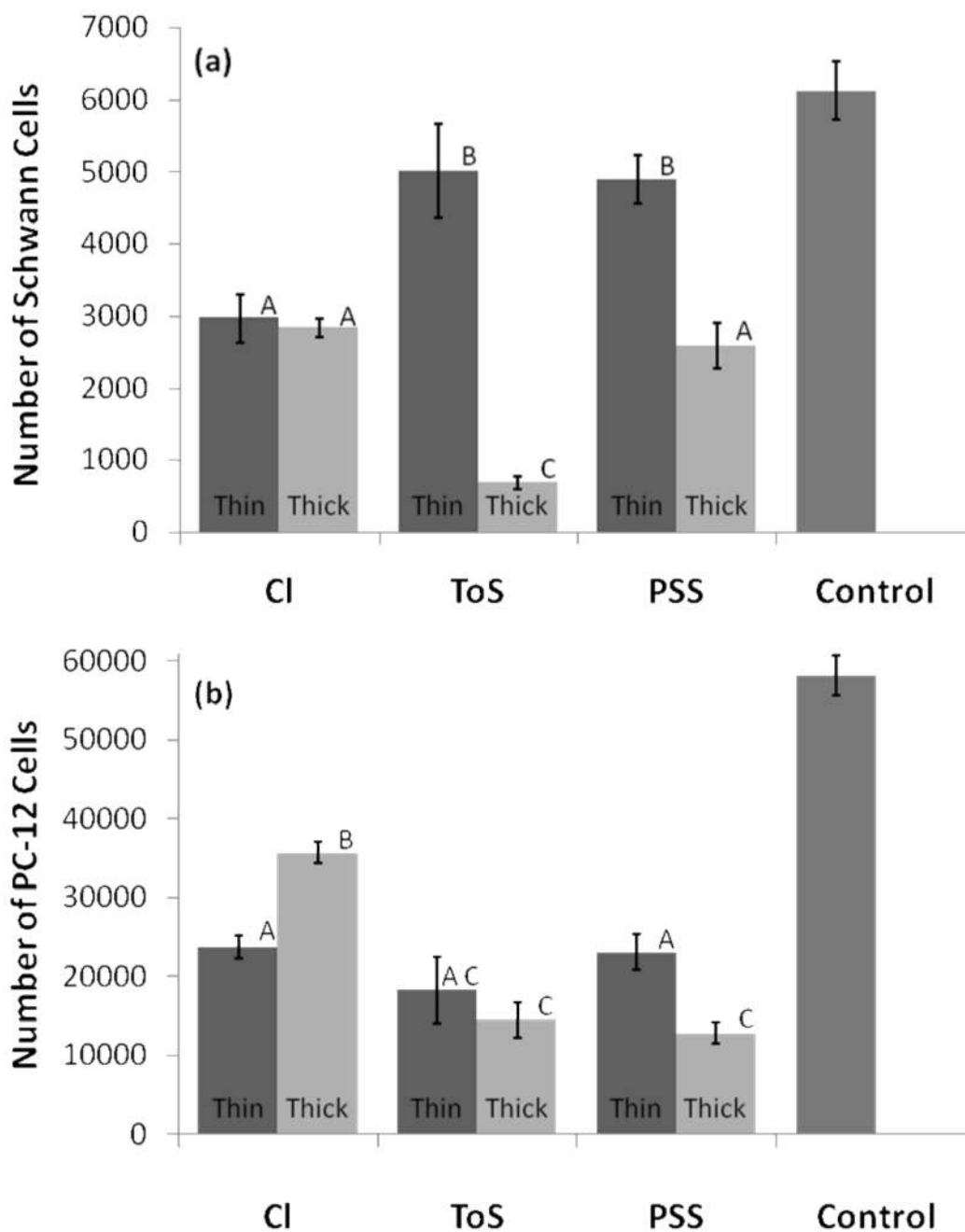


Figure 8. Cell Viability on Thick and Thin PPy Films

For all samples, Schwann (a) and PC-12 (b) cells were cultured for 24 hours on sterilized films. Viable cell numbers were calculated by luminescent ATP detection using a calibration curve. Regardless of the cell type used, ToS- and PSS-doped thick films (84 mC/cm^2) resulted in lower cell adhesion compared to their corresponding thin films (10.7 mC/cm^2 of charge passed). Thick chloride films performed as well or better than thin films, possibly because of changes in surface roughness. (a) Schwann cells cultured on thick and thin films of each dopant type (average \pm standard error). A PLL-coated plate was used as the positive control. Statistically significant groups are identified at the 0.05 level with different letters (A, B, or C) above each bar graph. $n = 16$. (b) PC-12 Cells cultured on thick and thin films of each dopant

type (average \pm standard error). A collagen-coated plate served as the positive control. Statistically significant groups are identified at the 0.05 level with different letters (A, B, or C) above each bar graph. n = 9.

Table 1
Relationship Between PPy Film Thickness and Charge Passed per Area

Dopant	Film Growth Rate on ITO Substrates (nm/mC/cm ³)	Film Growth Rate on Gold Substrates (nm/mC/cm ³)	Theoretical Film Growth Rate (nm/mC/cm ³)*
Cl	34.5	8.72	2.27
ToS	4.91	3.47	3.50
PSS	3.72	3.47	3.61

* Calculated from Equation [4] (Stankovic, *et al.* 1994).